Supporting Information for

Self-assembly of CdS_xSe_{1-x} Quantum Dots in Ryegrass

Li-Jiao Tian,[a] Nan-Qing Zhou,[a] Lin-Hui Yu,[b] Ting-Ting Zhu,[a] Wen-Wei Li,*[a] Peng-Fei An,[c] Jing-Yuan Ma,[d] Cheng-Bin Xiang,[b]

[a.]CAS Key Laboratory of Urban Pollutant Conversion, Department of Applied Chemistry, University of Science and Technology of China, Hefei, 230026, China

[b.]School of Life Sciences, University of Science and Technology of China, Hefei 230027, China

[c.]Beijing Synchrotron Radiation Laboratory, Institute of High Energy Physics, Chinese Academy of Science, Beijing, 100049, China

[d.]Shanghai Synchrotron Radiation Facility, Shanghai Institute of Applied Physics, Chinese Academy of Sciences, Shanghai 201204, China

This supporting information contains 18-page document, including materials and methods, 3 tables, 11 figures and this cover page.

MATERIALS AND METHODS

Plants Cultivation and QDs Biosynthesis. The QDs were assembled in *Lolium perenne* following the procedures shown in Fig. S1. The seeds were germinated in trays covered with gauze and moistened with water. The water was renewed every 3 days. After 2-week cultivation, for each test 18 ryegrass were transferred to 1/2 murashige and skoog (MS) medium in a 500-mL container, and thereafter were grown in a climate chamber at 24 °C with 70% humidity under alternate 16-h light and 8-h darkness. The solutions were renewed every 3 days. After cultivation for one month, the ryegrasses were transferred into a medium containing 1/2 MS salt and 100 μM Na_2SeO_4 for one day, followed by growing in another media with 1/2 MS salt, 100 μM Na_2SeO_4 and 800 μM $CdCl_2$ for two more days. For the Se-only group, the ryegrasses were transferred into a medium containing 1/2 MS salt and 100 μM Na_2SeO_4 for one day, followed by growing in another media with 1/2 MS salt, 100 μM Na_2SeO_4 for two more days. For the Cd-only group, the ryegrasses were transferred into a medium containing 1/2 MS salt and 800 μM $CdCl_2$ for two days. At last, the ryegrasses were collected, rinsed externally with millipore water to remove the absorbed ions. The harvested plant biomass was separated into different tissues (leaves, stems, and roots) and freeze-dried at 0.05 mbar and -20 °C for 24 h (FreeZone 2.5, Labconco Co., USA).

TEM Observation. For TEM analyses, samples were fixed overnight with 5% glutaraldehyde in 0.1 M phosphate buffer (pH 7.2). Fixed samples were dehydrated by step-wise increasing the contents of ethanol in deionized water (0%, 30%, 50%, 70%, 80%, 95%, 100%), and then were embedded in Spur resin. The embedded samples were cut into 100 nm sections using ultramicrotome (Leica EM UC7) and then transformed on copper grids with carbon coated. TEM (JEM-2011 JEOL Co., Japan) observation of the samples was conducted at 200 kV accelerating voltage.

Characterization of the Purified QDs. The washed ryegrass was re-suspended in 10 mM Tris-HCl (pH=7.6) buffer and disrupted by liquid nitrogen grinding. The broken liquid was filtered through 0.22-μm membrane. The filter liquor was transferred into a new centrifuge tube, and then centrifuged (15000 × g, 10 min) to collect the nanoparticles-containing supernatant. Then, the supernatant was added with proteinase K and incubated at 37 ^{o}C for 1 h. The resulting solution was centrifuged (15000 × g, 10 min) and washed 3 times using Amicon Ultra-15 50K centrifugal filter device. This QDs-rich solution was used for high-resolution transmission electron microscopy (HRTEM) analysis (2010F, JEOL Co., Japan), X-ray diffraction and XAFS measurements. The crystalline properties of the purified QDs were measured using X-ray diffraction beamline (BL14B1) of SSRF. The collecting range of 2θ was 10-70 degree.

XAFS Measurement. The dried ryegrass and purified nanoparticles were fixed on Kapton tape for XAFS analyses. Se XAFS were measured at the beamline 1W1B of Beijing Synchrotron Radiation Facility (BSRF), China. Cd *K*-edge XAFS were recorded at the beamline BL14W1 of Shanghai Synchrotron Radiation Facility (SSRF). The XAFS were collected and analysed following our reported work.[1]

XANES **Analyses.** The sample XANES spectra were quantitatively analyzed by linear combination fitting (LCF) based on the standard spectra of CdSe, Na_2SeO_4, Na_2SeO_3, seleno-L-methionine and Se^0. In light of the similarity of organo-Se species (e.g., Se-methionine and Se-cysteine) in their XAS spectra, seleno-L-methionine was used as the reference for organo-Se compounds. LCF was performed over the energy range 12645 to 12700 eV. Individual LCF fractions were constrained to a range between 0 and 1, and the sum of all fractions was set as 1.

EXAFS Analyses. All the curve-fittings were performed using the ARTEMIS module implemented in the IFEFFIT package. In Se curve fittings, the amplitude reduction factor S_0^2 was fixed at 0.8 as determined by fitting the data of CdSe standard. Fittings were conducted in the R-space for k^3-weighted $\chi(k)$ functions with Hanning windows (dk = 1.0 $Å^{-1}$). For the root sample, a k-range of 2.8-13.7 $Å^{-1}$ and R-range of 1.2-2.8 Å was used. For the stem sample, a k-range of 2.7-11.5 $Å^{-1}$ and R-range of 1.2-2.8 Å was used. For the leave sample, a k-range of 3-12 $Å^{-1}$ and R-range of 1.1-2.8 Å was used. According to the reported articles,[2, 3] the samples have been fitted together with same Debye-Waller factors (σ^2) and energy shift (ΔE_0) to reduce the number of adjustable parameters. Therefore the number of independent points for these three samples when fitting together are $N_{ipt} = (2\Delta k \cdot \Delta R/\pi)_{root} + (2\Delta k \cdot \Delta R/\pi)_{stem} + (2\Delta k \cdot \Delta R/\pi)_{leave} = 2\times(13.7-2.8)\times(2.8-1.2)/\pi + 2\times(11.5-2.7)\times(2.8-1.2)/\pi + 2\times(12-3)\times(2.8-1.1)/\pi = 29$. The number of adjustable parameters in the fits is 28, less than N_{ipt} (29).

In Cd curve fittings, the amplitude reduction factor S_0^2 was fixed at a value of 0.8 as determined by fitting the data of CdSe standard. Fittings were performed in the R-space for k^3-weighted $\chi(k)$ functions with Hanning windows (dk = 1.0 $Å^{-1}$). For the root sample, a k-range of 2.1-9.5 $Å^{-1}$ and R-range of 1-2.8 Å was used. For the stem sample, a k-range of 2.1-9.2 $Å^{-1}$ and R-range of 1.1-2.9 Å was used. For the leave sample, a k-range of 2.3-9.8 $Å^{-1}$ and R-range of 1-2.8 Å was used. The samples were fitted together with same Debye-Waller factors (σ^2) and energy shift (ΔE_0) to reduce the number of adjustable parameters. Therefore, the number of independent points for the three samples when fitting together was $N_{ipt} = (2\Delta k \cdot \Delta R/\pi)_{root} + (2\Delta k \cdot \Delta R/\pi)_{stem} + (2\Delta k \cdot \Delta R/\pi)_{leave} = 2\times(9.5-2.1)\times(2.8-1)/\pi + 2\times(9.2-2.1)\times(2.9-1.1)/\pi + 2\times(9.8-2.3)\times(2.8-1)/\pi = 24$. The number of adjustable parameters in the fits was 16, less than N_{ipt} (24).

μ-SXRF Mapping. The washed tissues of ryegrass were cut into ~3 cm sections, and placed between two pieces of Kapton polyimide film. The samples were rapidly frozen in liquid nitrogen and freeze-dried with vacuum freeze dryer (FreeZone 2.5, Labconco Co., USA). The μ-SXRF mapping of the above prepared samples was analysed at the BL-15U1 beamline of SSRF following our previously work.[4]

Fluorescence Microscope Observation. The washed roots were loaded on a glass slide for fluorescence observation. Fluorescence images were taken by a wide field fluorescent microscope (BX-51, Olympus Co., Japan) under 120 W mercury lamp (X-Cite 120 Q) irradiation, and recorded using DP2-BSW software (Olympus Co., Japan). The lamp was equipped with a wideband MWU2 filter (Ex 330-385 nm) and a water immersion objective (10×).

Cd Spatial Distribution. The distribution of Cd in ryegrass after exposure to Na_2SeO_4 and $CdCl_2$ for 2 days was visualized using Cd specific probe Leadmium™ Green AM (Invitrogen, Carlsad, CA, USA). According to the manufacture's instructions, the washed roots and leaves were immersed in the dye solution at 37 °C for 4 h in the dark, then washed with 0.85 % NaCl three times prior to fluorescence microscopic examination.

Table S1. Linear Combination Fitting Analyses of the XANES Spectra

Samples	CdSe	Na_2SeO_4	organo-Se	Se^0
Root - purified from Cd & Se treated	40	3	50	7
Stem - purified from Cd & Se treated	28	0	65	7
Leave - purified from Cd & Se treated	24	4	70	2

Table S2. Se *K*-edge EXAFS Curve Fitting Parameters[a]

Samples	Shell	*N*	*R* (Å)	σ^2 (Å^2)	ΔE_0 (eV)	*R* (%)
Se[b]	Se-Se	**2**	2.38 (1)	0.004 (1)	6.9 (4)	0.1
CdSe[b]	Se-Cd	**4**	2.62 (1)	0.005 (1)	2.8 (4)	0.1
Na_2SeO_3[b]	Se-O	**3**	1.70 (1)	0.002 (3)	8.9 (5)	0.7
SeMet[b]	Se-C	**6**	1.96 (1)	0.002 (4)	8.7 (7)	0.9
Root[c]	Se-Se	0.3 (1)	2.35 (1)	0.004 (2)	2.0 (8)	1.2
	Se-Cd	1.8 (4)	2.61 (1)	0.005 (1)	2.2 (2)	
	Se-C	1.5 (3)	1.89 (3)	0.003 (1)	8.7 (7)	
Stem[d]	Se-Se	0.3 (1)	2.36 (4)	0.004 (2)	2.0 (8)	1.2
	Se-Cd	1.5 (3)	2.61 (2)	0.005 (1)	2.2 (2)	
	Se-C	2.1 (4)	1.89 (3)	0.003 (4)	8.7 (7)	
Leave[e]	Se-Se	0.2 (4)	2.39 (9)	0.004 (6)	2.0 (8)	1.2
	Se-Cd	0.8 (6)	2.60(1)	0.005 (2)	2.2 (2)	
	Se-C	3.7 (4)	1.92 (4)	0.003 (4)	8.7 (7)	
	Se-O	1.3 (6)	1.75 (2)	0.003 (5)	8.3 (4)	

[a]*N*, coordination number; *R*, distance between absorber and backscatter atoms; σ^2, Debye–Waller factor to account for both thermal and structural disorders; ΔE_0, the shift of the energy threshold; *R* factor (%) indicates the goodness of the fit. Errors are given in brackets. S_0^2 was fixed to 0.8 as determined from CdSe standard fitting. Bold numbers indicate fixed coordination number (*N*) according to the crystal structure. [b] The same as in our previous work.[5] [c] Fitting range: $2.8 \leq k$ (/Å) ≤ 13.7 and $1.2 \leq R$ (Å) ≤ 2.8. [d] Fitting range: $2.7 \leq k$ (/Å) ≤ 11.5 and $1.2 \leq R$ (Å) ≤ 2.8. [e] Fitting range: $3 \leq k$ (/Å) ≤ 12 and $1.1 \leq R$ (Å) ≤ 2.8.

Table S3. Cd *K*-edge EXAFS Curve Fitting Parameters[a] obtained with two atomic shells

Samples	Shell	*N*	*R* (Å)	σ^2 (Å^2)	ΔE_0 (eV)	*R* (%)
CdO[b]	Cd-O	**6**	2.32 (1)	0.008 (1)	1.0 (7)	1.5
CdS[c]	Cd-S	**4**	2.52 (1)	0.006 (1)	1.9 (5)	0.1
CdSe[d]	Cd-Se	**4**	2.63 (1)	0.006 (1)	3.0 (6)	0.1
$Cd_3(PO_4)_2$[e]	Cd-O	6.6 (5)	2.28 (2)	0.011 (1)	3.3 (9)	0.3
Root[f]	Cd-S Cd-O	0.7 (5) 3.6 (6)	2.49 (2) 2.24 (3)	0.003 (4) 0.008 (3)	3.8 (5) 5.6 (5)	1.5
Stem[g]	Cd-S Cd-O	1.6 (5) 2.3 (6)	2.48 (3) 2.25 (5)	0.003 (4) 0.008 (3)	3.8 (5) 5.6 (5)	1.5
Leave[h]	Cd-S	2.3 (5)	2.46 (4)	0.003 (4)	3.8 (5)	1.5

[a] *N*, coordination number; *R*, distance between absorber and backscatter atoms; σ^2, Debye–Waller factor to account for both thermal and structural disorders; ΔE_0, the shift of the energy threshold; *R* factor (%) indicates the goodness of the fit. Errors are given in brackets. S_0^2 was fixed to 0.8 as determined from CdSe standard fitting. Bold numbers indicate fixed coordination number (*N*) according to the crystal structure. [b] The same as in our previous work. [c] Fitting range: $3 \le k$ (/Å) ≤ 11 and $1.15 \le R$ (Å) ≤ 3. [d] Fitting range: $3 \le k$ (/Å) ≤ 10.7 and $1.1 \le R$ (Å) ≤ 2.9. [e] Fitting range: $3 \le k$ (/Å) ≤ 11 and $1.1 \le R$ (Å) ≤ 2.9. [f] Fitting range: $2.1 \le k$ (/Å) ≤ 9.5 and $1 \le R$ (Å) ≤ 2.8. [g] Fitting range: $2.1 \le k$ (/Å) ≤ 9.2 and $1.1 \le R$ (Å) ≤ 2.9. [h] Fitting range: $2.3 \le k$ (/Å) ≤ 9.8 and $1 \le R$ (Å) ≤ 2.8.

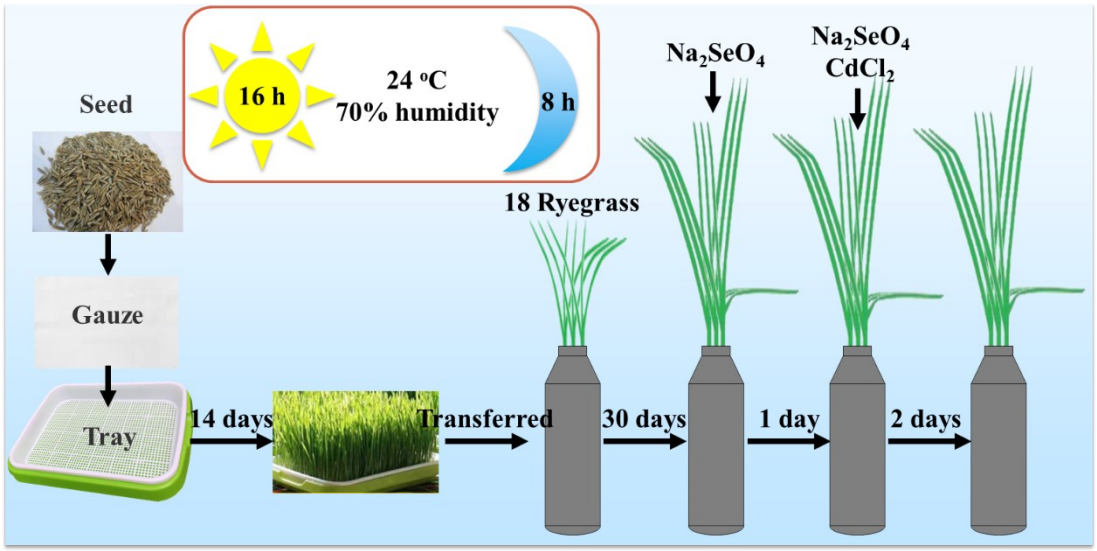

Fig. S1 Diagram of the experimental procedures for the nanoparticles biosynthesis in ryegrass.

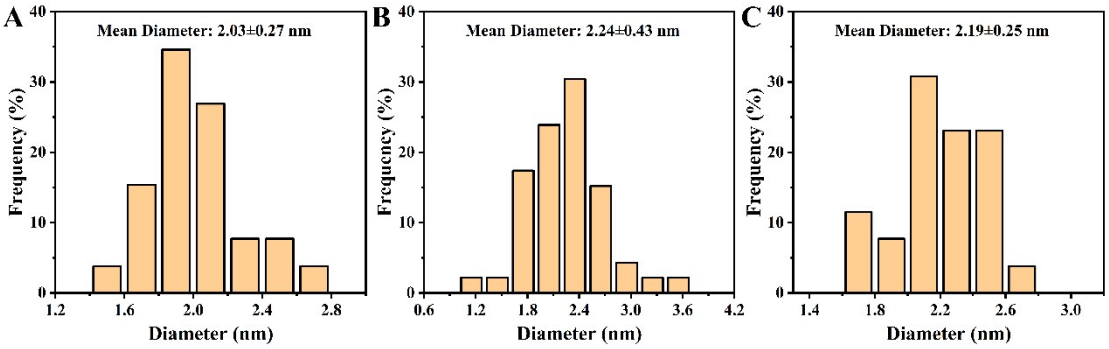

Fig. S2 Size distribution of the purified nanoparticles form leaves (A), stems (C) and roots (C).

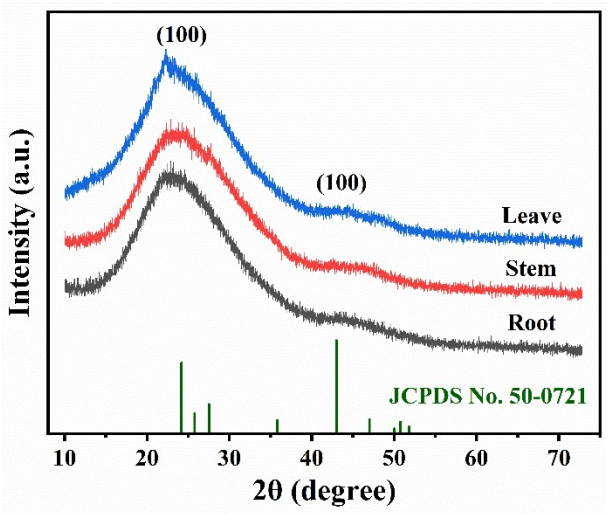

Fig. S3 X-ray Diffractometer (XRD) patterns of the purified nanoparticles from leaves, stems and roots.

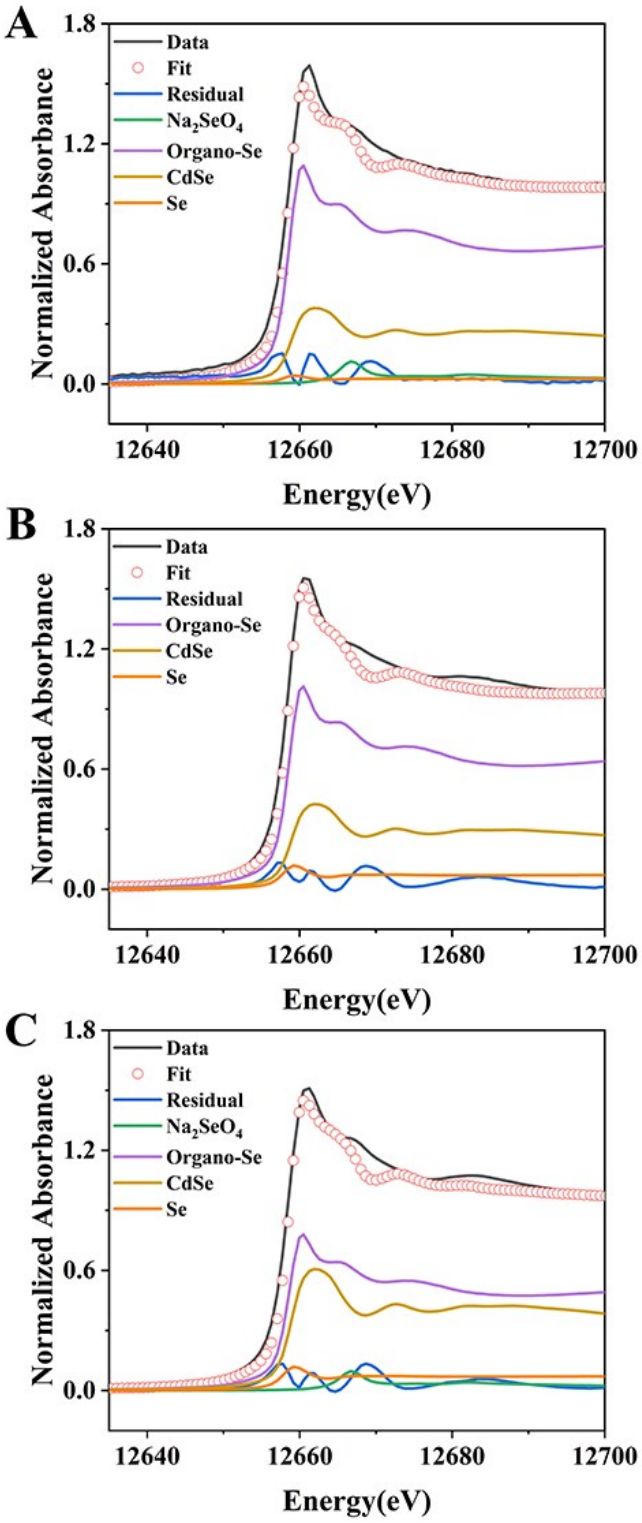

Fig. S4 LCF results of Se XANES spectra of the purified samples from the leaves (A), stems (B) and roots(C) of the plants treated with Se and Cd.

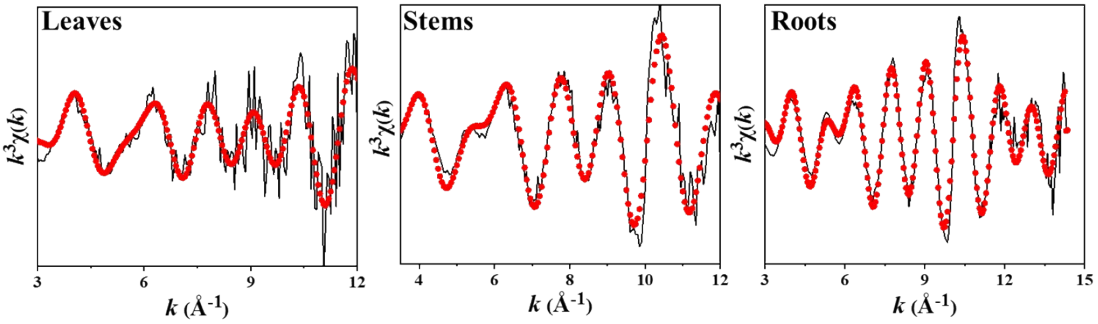

Fig. S5 Se *K*-edge EXAFS analyses of the purified samples from the roots, stems and leaves of ryegrass in *k* spaces. The theoretical signals (red circle) are superimposed on the experimental one (black line) using the ARTEMIS software. Measured spectra matched with the calculated data very well. The best-fit parameters are shown in Table S2.

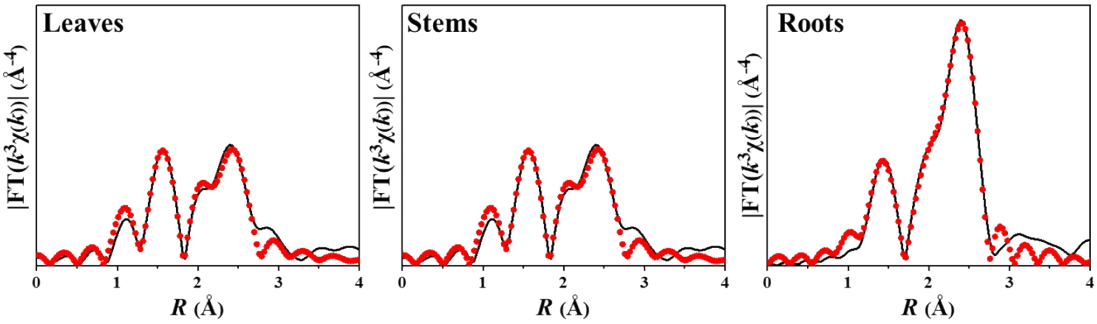

Fig. S6 Fourier-transformed magnitudes of Se *K*-edge EXAFS spectra in *R* space for the purified samples from the roots, stems and leaves of ryegrass using the ARTEMIS software. Measured spectra (black line) matched with the calculated data (red circle) very well for all standards. The best-fit parameters are shown in Table S2.

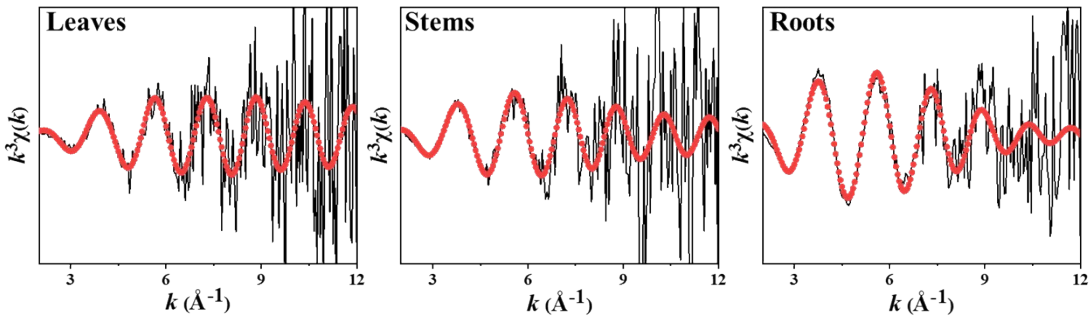

Fig. S7 Cd *K*-edge EXAFS analysis of the purified samples from the roots, stems and leaves of ryegrass in *k* spaces. The samples were fitted with Cd-S and Cd-O two paths. The theoretical signals (red circle) are superimposed on the experimental one (black line). The best-fit parameters are shown in Table S3.

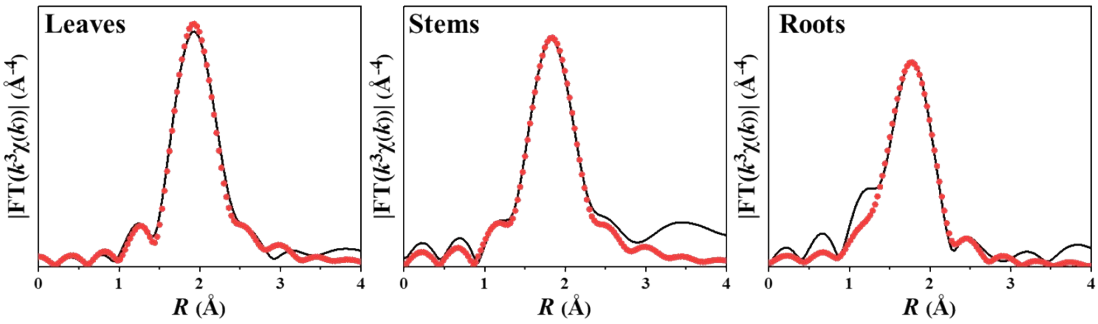

Fig. S8 Fourier-transformed magnitudes of Cd *K*-edge EXAFS analysis of the purified samples from the roots, stems and leaves of ryegrass in *R* space. The samples were fitted with Cd-S and Cd-O two paths. The theoretical signals (red circle) are superimposed on the experimental one (black line). The best-fit parameters are shown in Table S3.

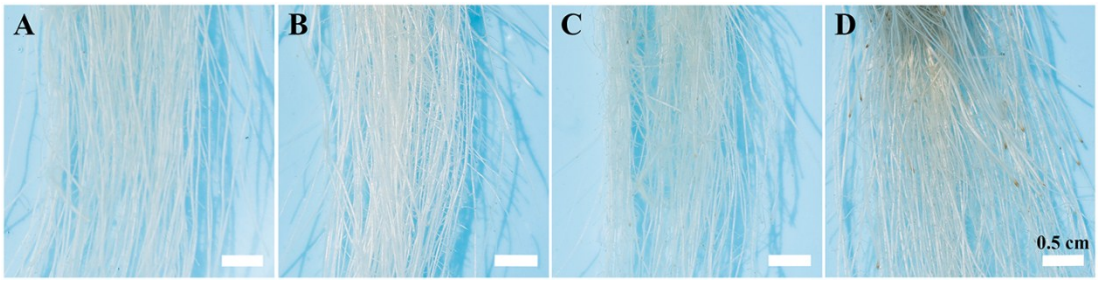

Fig. S9 Bright field images of the ryegrass under different treatment regimes of Se and Cd, including Blank (A), Na_2SeO_4 only (B), $CdCl_2$ only (C) and Na_2SeO_4 & $CdCl_2$ (D).

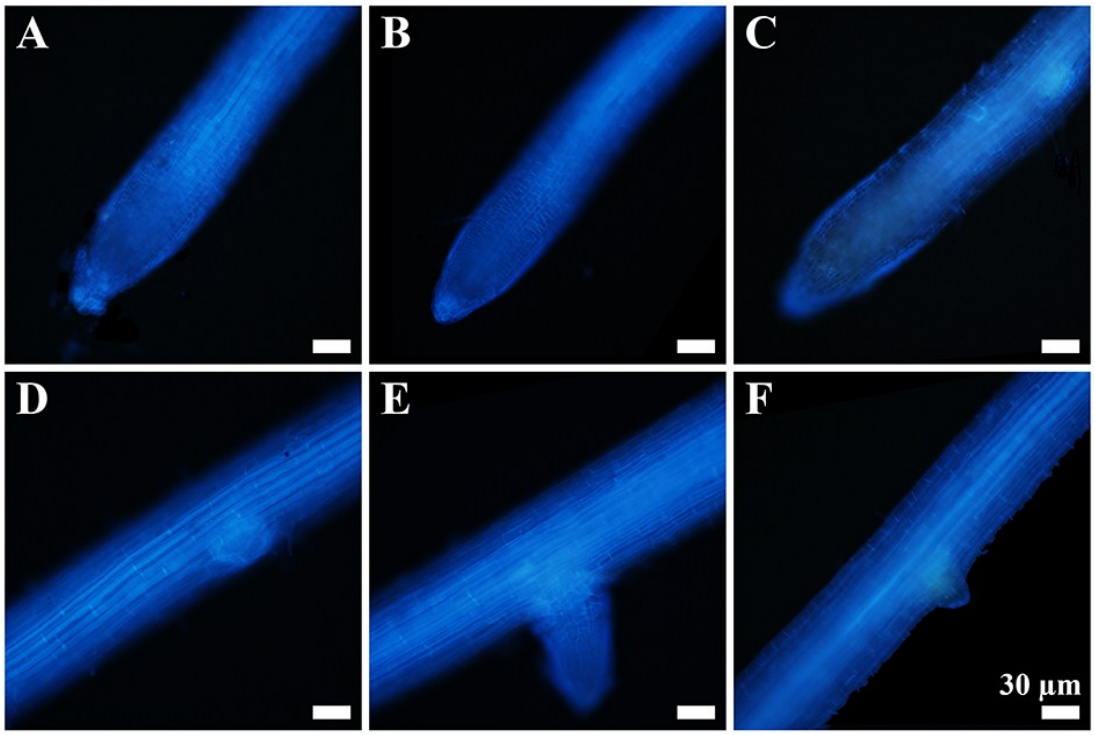

Fig. S10 Fluorescence images of the ryegrass roots under different treatment regimes of Se and Cd, including Blank (A, D), Na_2SeO_4 only (B, E), $CdCl_2$ only (C, F). All images were collected under the same exposure conditions.

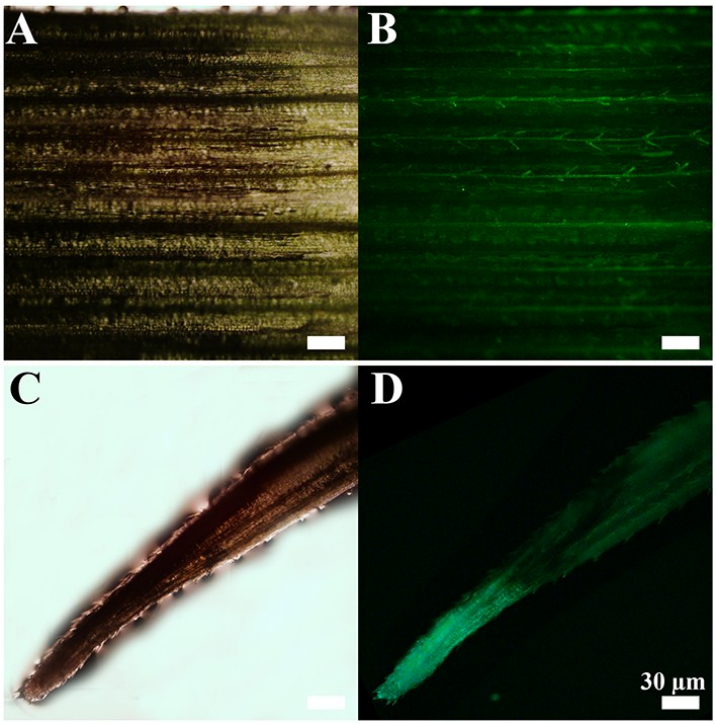

Fig. S11 Bright field images (A, C) and fluorescence microscopy images (B, D) of the ryegrass leaves with Cd probe staining. The green fluorescence intensity represents the Cd content.

REFERENCES

1. L. J. Tian, Y. Min, W. W. Li, J. J. Chen, N. Q. Zhou, T. T. Zhu, D. B. Li, J. Y. Ma, P. F. An, L. R. Zheng, H. Huang, Y. Z. Liu and H. Q. Yu, *ACS Nano*, 2019, **13**, 5841-5851.
2. A. I. Frenkel, E. A. Stern, M. Qian and M. Newville, *Phys. Rev. B Condens. Matter*, 1993, **48**, 12449-12458.
3. S. Wei and Z. Sun, *J. Phys-Condens. Mat.*, 2005, **17**, 8017-8028.
4. L. L. Li, Y. H. Cui, L. Y. Lu, Y. L. Liu, C. J. Zhu, L. J. Tian, W. W. Li, X. Zhang, H. Cheng, J. Y. Ma, J. Chu, Z. H. Tong and H. Q. Yu, *Environ. Sci. Technol.*, 2019, **53**, 2344-2352.
5. L. J. Tian, W. W. Li, T. T. Zhu, J. J. Chen, W. K. Wang, P. F. An, L. Zhang, J. C. Dong, Y. Guan, D. F. Liu, N. Q. Zhou, G. Liu, Y. C. Tian and H. Q. Yu, *J. Am. Chem. Soc.*, 2017, **139**, 12149-12152.